Meflin is a marker of pancreatic stellate cells involved in fibrosis and epithelial regeneration in the pancreas

Ryota Ando,[1] Yukihiro Shiraki,[1] Yuki Miyai,[1] Hiroki Shimizu,[1] Kazuhiro Furuhashi,[2] Shun Minatoguchi,[2] Katsuhiro Kato,[3] Akira Kato,[1] Tadashi Iida,[1] Yasuyuki Mizutani,[1] Kisuke Ito,[1] Naoya Asai,[4] Shinji Mii,[1] Nobutoshi Esaki,[1] Masahide Takahashi,[5] Atsushi Enomoto[1,6]

[1]Department of Pathology, [2]Nephrology, and [3]Cardiology, Nagoya University Graduate School of Medicine, Nagoya, Japan

[4]Department of Molecular Pathology and [5]Division of International Center for Cell and Gene Therapy, Fujita Health University, Toyoake, Japan

[6]Center for One Medicine Innovative Translational Research, Gifu University Institute for Advanced Study, Gifu Japan

Correspondence: Atsushi Enomoto, Department of Pathology, Nagoya University Graduate School of Medicine, 65 Tsurumai-Cho, Showa-Ku, Nagoya 466-8550, Japan; Tel: +81-52-744-2093; Fax: +81-52-744-2098; Email: enomoto@iar.nagoya-u.ac.jp

Conflicts of interest: The authors declare no conflicts of interest.

Running title: Meflin is a PSC marker

Word count: 4346 words

Abstract

Pancreatic stellate cells (PSCs) are stromal cells in the pancreas that play an important role in pancreatic pathology. In chronic pancreatitis (CP) and pancreatic ductal adenocarcinoma (PDAC), PSCs are known to get activated to form myofibroblasts or cancer-associated fibroblasts (CAFs) that promote stromal fibroinflammatory reactions. However, previous studies on PSCs were mainly based on the findings obtained using *ex vivo* expanded PSCs, with few studies that addressed the significance of *in situ* tissue-resident PSCs using animal models. Their contributions to fibrotic reactions in CP and PDAC are also lesser-known. These limitations in our understanding of PSC biology have been attributed to the lack of specific molecular markers of PSCs. Herein, we established Meflin (*Islr*), a glycosylphosphatidylinositol-anchored membrane protein, as a PSC-specific marker in both mouse and human by using human pancreatic tissue samples and Meflin reporter mice. Meflin-positive (Meflin$^+$) cells contain lipid droplets and express the conventional PSC marker Desmin in normal mouse pancreas, with some cells also positive for Gli1, the marker of pancreatic tissue-resident fibroblasts. Three-dimensional analysis of the cleared pancreas of Meflin reporter mice showed that Meflin$^+$ PSCs have long and thin cytoplasmic protrusions, and are localised on the abluminal side of vessels in the normal pancreas. Lineage tracing experiments revealed that Meflin$^+$ PSCs constitute one of the origins of fibroblasts and CAFs in CP and PDAC, respectively. In these diseases, Meflin$^+$ PSC-derived fibroblasts showed distinctive morphology and distribution from Meflin$^+$ PSCs in the normal pancreas. Furthermore, we showed that the genetic depletion of Meflin$^+$ PSCs accelerated fibrosis and attenuated epithelial regeneration and stromal R-spondin 3 expression, thereby implying that Meflin$^+$ PSCs and their lineage cells may support tissue recovery and Wnt/R-spondin signalling after pancreatic injury and PDAC development. Together, these data indicate that Meflin may be a marker specific to tissue-resident PSCs and useful for studying their biology in both health and disease.

Keywords: pancreas, fibrosis, chronic pancreatitis, pancreatic ductal adenocarcinoma, pancreatic stellate cell, fibroblast, cancer-associated fibroblast, Meflin, Islr.

Introduction

Pancreatic stellate cells (PSCs) are key players in the physiology and pathology of the pancreas [1–3]. In normal healthy pancreas, PSCs are pericyte- or fibroblast-like stromal cells characterised by cytoplasmic lipid droplets in their quiescent state [4–7]. PSCs are activated in chronic pancreatitis (CP) and pancreatic ductal adenocarcinoma (PDAC) to promote fibroinflammatory reactions in the stroma, which are hallmarks of these diseases [8,9]. Fibrosis remarkably contributes to disease progression and therapy resistance in pancreatic disease [10–12]; therefore, elucidating PSC functions may provide a more comprehensive understanding of the pathogenesis and novel therapeutic strategies for diseases.

Integrating the data obtained from *ex vivo* expanded PSCs and extrapolating them to the role of PSCs *in vivo* is a major challenge in the field of PSC research [3,13,14]. Since the development of methods to isolate PSCs, many studies have identified the critical roles of PSCs in both normal and diseased pancreas [6,7]. However, few studies have directly examined the *in situ* functions of PSCs through experiments, using genetically engineered mouse models that allow us to track and manipulate PSCs [13,14]. In particular, the precise contribution of PSCs to fibrotic reactions in diseases remains unclear due to the lack of PSC-specific molecular markers that can be applied to the Cre-loxP-mediated recombination system [14,15]. Conventional PSC markers, such as Desmin and glial fibrillary acidic protein (GFAP), have limitations in specificity, species dependence, and usability for *in vivo* experiments [13,14,16].

The present study established Meflin, a glycosyl-phosphatidylinositol-anchored membrane protein encoded by the immunoglobulin superfamily containing leucine-rich repeat (*Islr*) gene [17], as a PSC marker. Meflin is expressed by stromal cells of the normal pancreas and cancer-associated fibroblasts (CAFs) in PDAC, suggesting that Meflin is a potential PSC marker [18–22]. Using this new PSC marker, we observed, traced, and depleted PSCs in both normal and diseased pancreas *in vivo*. Our results provide evidence that Meflin-positive (Meflin^{+}) PSCs constitute one of the origins of fibroblasts in CP and PDAC, and illustrate the

distinctive morphologies and distributions in normal and diseased pancreas and their involvement in tissue recovery after pancreatic injury.

Methods

Human tissue samples

Normal human pancreatic tissue was obtained from the normal part of formalin-fixed paraffin-embedded (FFPE) samples from a patient who had undergone surgery for PDAC at Nagoya University Hospital. This study was approved by the ethics committee of Nagoya University Graduate School of Medicine (approval number 2017-0127-4).

Mice

Meflin-CreERT2 knock-in mice expressing tamoxifen-inducible Cre recombinase under the Meflin promoter, Meflin-ZsGreen-t2a-DTR-t2a-Cre (ZDC) knock-in mice that simultaneously express ZsGreen, diphtheria toxin receptor (DTR), and constitutively active Cre recombinase under the Meflin promoter, and Meflin-knockout (KO) mice were previously generated in our laboratory [17,18,23]. Fluorescent reporter mice, Rosa26-loxP-stop-loxP (LSL)-tdTomato mice (7909, Jackson Laboratory, Bar Harbor, ME, USA), and Rosa26-loxP-stop-loxP (LSL)-mTmG mice (7676, Jackson Laboratory) were used for lineage tracing and imaging analyses. All mice were maintained on the C57BL/6J background (Charles River Laboratories Japan, Yokohama, Japan). Male or female 8–15-week-old mice were used in this study. All mice were kept in autoclaved cages and provided with sterile drinking water and chow *ad libitum*. A priori power calculations were not performed to predetermine the sample size for the mouse experiments. Mice were randomly assigned to groups. The investigators were not blinded to the allocation during the experiments and outcome assessments. All animal protocols were approved by the animal care and use

committee of the Nagoya University Graduate School of Medicine (approval number M220014-006).

Detailed protocols for animal experiments, histology, imaging analyses, cell culture, and statistical analyses are described in the Supplementary materials.

Results

Meflin is expressed in stromal cells of both mouse and human pancreas

We first compared the expression of *Islr* mRNA (hereafter referred to as *Islr*) and Desmin, a conventional rodent PSC marker [6,7]. *In situ* hybridisation (ISH) assay detected *Islr* in stromal cells localised around pancreatic acini, small interlobular ducts, and islets in the mouse pancreas (**Figure 1A**). Immunohistochemistry (IHC) revealed that the distribution of *Islr*$^+$ stromal cells was remarkably similar to that of Desmin$^+$ stromal cells (**Figure 1A**). However, Desmin was not specific to those stromal cells and was robustly expressed in vascular smooth muscle cells. Double staining of *Islr* and Desmin by ISH and immunofluorescence (IF), respectively, showed that approximately 70–75% of Desmin$^+$ cells expressed *Islr* (**Figure 1B, C**). Most Desmin$^+$ *Islr*$^-$ cells appeared to be vascular smooth muscle cells of small- and mid-sized vessels (**Supplementary material, Figure S1A**). In addition, *Islr*$^+$ Desmin$^-$ cells were observed, suggesting the heterogeneity of pancreatic stromal cells in terms of gene expression.

Next, we isolated PSCs from adult mouse pancreas by collagenase disaggregation and density gradient centrifugation using Histodenz [6,24], followed by culture on plastic plates for 24 hours and ISH for *Islr* expression (**Figure 1D, Supplementary material, S1B**). The data showed that approximately 40% of the isolated PSCs were positive for *Islr* (**Figure 1E**). The purity of the collected PSCs was about 60–70%, as evaluated by the presence of

cytoplasmic lipid droplets, detected by staining with the lipophilic fluorescent probe BODIPY 493/503 or the positivity of Desmin detected by IF staining (**Figure 1E, Supplementary material, S1B**). These data suggested that approximately 60% of PSCs expressed *Islr* in the mouse pancreas. The specific expression of Meflin in PSCs was also supported by the analysis of a publicly available database of single-cell transcriptomic analysis of normal mouse pancreas [18,25]. The results revealed that *Islr*$^{+}$ cells did not overlap with cell populations that were positive for epithelial markers (*Epcam*, *Cdh1*), vascular endothelial markers (*Cdh5*, *Pecam1*), or a leukocyte marker (*Ptprc*) (**Supplementary material, Figure S1C**).

In the human pancreas, we detected Meflin expression in stromal cells localised around the pancreatic acini at both the mRNA and protein levels (**Figure 1F**). *ISLR* was not detected in E-cadherin^{+} epithelial cells, thereby supporting the specificity of Meflin expression in stromal cells (**Supplementary material, Figure S1D**). In contrast, Desmin was preferentially expressed in vascular smooth muscle cells, but not in any stromal cells (**Figure 1F**), consistent with a previous study which showed that Desmin is not useful as a human PSC marker [16]. These results suggest that Meflin is a universal PSC marker conserved across species.

Meflin-CreERT2 knock-in mouse specifically labels PSCs

To further characterise and visualise Meflin^{+} cells *in vivo*, we used Meflin reporter mice previously generated by crossing Rosa26-loxP-stop-loxP (LSL)-tdTomato reporter mice with Meflin-CreERT2 knock-in mice that express tamoxifen-inducible Cre recombinase under the control of the Meflin promoter (hereafter referred to as Meflin-CreERT2; LSL-tdTomato mice) [18]. Six-week-old Meflin-CreERT2; LSL-tdTomato mice were orally administered tamoxifen, followed by the visualisation of tdTomato^{+} cells in the pancreas by IHC or IF at eight weeks old (**Figure 2A**). We found tdTomato^{+} cells around the pancreatic acini, ducts, and islets, consistent with endogenous *Islr* expression (**Figure 2B**). We confirmed reporter

fidelity by double staining of *Islr* and tdTomato protein using ISH and IF, respectively (**Figure 2C–E**). The results showed that most tdTomato$^+$ cells were positive for *Islr*, confirming the specificity of the mice to reflect endogenous *Islr* expression (**Figure 2D**). The efficiency of tdTomato labelling in *Islr*$^+$ cells was approximately 25% (**Figure 2E**).

To validate Meflin as a PSC marker, we examined the expression of other cellular markers and the presence of lipid droplets in tdTomato$^+$ cells of the Meflin-CreERT2; LSL-tdTomato mice (**Figure 2F–I**). Double IF staining showed that most tdTomato$^+$ cells were positive for Desmin, but negative for pan-epithelial cell marker E-cadherin, smooth muscle cell marker α-smooth muscle actin (α-SMA), and vascular endothelial marker CD31 (**Figure 2F, G**). Interestingly, there was a small number of tdTomato and α-SMA double-positive cells intercalated between the smooth muscle layers of vessels, which was also supported by double staining for *Islr* mRNA and α-SMA protein (**Supplementary material, Figure S2A, B**). Importantly, most tdTomato$^+$ cells that were dissociated from the pancreas possessed cytoplasmic lipid droplets, visualised using BODIPY 493/503 (**Figure 2H, I**). Additionally, we attempted to detect the intracellular accumulation of retinol, which is another hallmark of PSCs, by exciting its autofluorescence with ultraviolet (UV) [1,4,6]. Although we could not observe UV-excited autofluorescence in cultured tdTomato$^+$ cells, presumably due to the very low retinol content in mouse PSCs as reported [26], we observed the accumulation of retinol in tdTomato$^+$ cells when they were preloaded with exogenous retinol, thus suggesting that they are competent for extracellular retinol uptake (**Supplementary material, Figure S3**). Based on these findings, we posited that Meflin acts as a marker for at least some PSC populations and that the Meflin-CreERT2; LSL-tdTomato mouse is a useful mouse model for monitoring Meflin$^+$ PSCs and their offspring.

Fatty acid-binding protein 4 (Fabp4) has been proposed to be a PSC marker [27,28]; therefore, we compared Meflin expression with that of Fabp4 in the mouse pancreas (**Figure 2J, K**). tdTomato$^+$ cells showed no evident expression of Fabp4 protein, suggesting that Meflin$^+$ PSCs represent a distinct PSC subset from Fapb4$^+$ cells in mouse pancreas. Other important stromal cells in the pancreas are tissue-resident fibroblasts positive for the GLI

family zinc finger (*Gli1*) transcription factor, which expand upon pancreatitis and PDAC induction [29]. Double ISH for endogenous *Islr* and *Gli1* showed that approximately 25% of *Islr*$^+$ cells were positive for *Gli1,* whereas most *Gli1*$^+$ cells expressed *Islr* (**Figure 2L, M**). Despite the methodological limitation that detection sensitivity varies between methods, such as IF, ISH, and reporter mice, the data suggested that Meflin indicates a more broadly inclusive and heterogeneous population of PSCs or fibroblasts in mouse pancreas that are not Fabp4-positive (**Figure 2N**).

Since PSCs are considered as counterparts of hepatic stellate cells (HSCs) [30], we also examined the localisation of Meflin$^+$ cells in the normal mouse liver. Interestingly, we found that the distribution of tdTomato$^+$ cells was distinct from that of HSCs labelled with Desmin or GFAP [31] in the liver of Meflin-CreERT2; Rosa-LSL-tdTomato mice (**Supplementary material, Figure S4A–C**); while HSCs were scattered in the intralobular stromal compartment, tdTomato$^+$ cells were predominantly located around the portal venules. Furthermore, using double ISH for *Islr* and nerve growth factor receptor (*Ngfr*), another HSC-specific marker [31], we found limited overlap between *Islr*$^+$ cells and *Ngfr*$^+$ HSCs (**Supplementary material, Figure S4D, E**). These results suggest that Meflin labels fibroblastic stromal cells that are distinct from the majority of HSCs.

Meflin-constitutive Cre knock-in mouse labels PSCs

To examine the involvement of Meflin lineage cells labelled during embryonic development and postnatal maturation of the pancreas, we crossed Meflin-ZDC mice [23] with Rosa26-LSL-tdTomato reporter mice (hereafter termed Meflin-ZDC; LSL-tdTomato mice) (**Supplementary material, Figure S5A**). Meflin-ZDC mice express the green fluorescent protein ZsGreen (Z), diphtheria toxin receptor (D), and constitutively active Cre recombinase (C) under the Meflin promoter. In Meflin-ZDC; LSL-tdTomato mice, any cells that once expressed Meflin should express tdTomato irreversibly, thus helping to trace and localise Meflin lineage cells. IHC for tdTomato in tissue sections prepared from the pancreas of adult

Meflin-ZDC; LSL-tdTomato mice showed the presence of tdTomato$^+$ stromal cells in the periacinar and periductal regions (**Supplementary material, Figure S5B**). Surprisingly, double staining for tdTomato by IF and *Islr* mRNA by ISH revealed that almost all tdTomato$^+$ Meflin lineage cells were positive for *Islr* mRNA (**Supplementary material, Figure S5C, D**). In addition, most tdTomato$^+$ cells expressed Desmin, but not CD31 or E-cadherin (**Supplementary material, Figure S5E, F**). These data indicate that Meflin lineage cells do not produce endothelial and epithelial cells throughout development and adult life. Interestingly, approximately 12% of tdTomato$^+$ cells were α-SMA$^+$ smooth muscle cells localised on the abluminal side of vessels. These data suggested that most Meflin lineage cells remain as Meflin$^+$ PSCs, and their minor fraction contributes to α-SMA$^+$ perivascular cells or smooth muscle cells during embryonic development or later in life.

Meflin$^+$ PSCs are located along the vasculature with long cytoplasmic protrusions in normal pancreas

Since most Meflin lineage cells represent PSCs actively expressing Meflin (**Supplementary material, Figure S5C, D**), we examined the morphology of those Meflin$^+$ cells using Meflin-ZDC mice crossed with Rosa26-loxP-stop-loxP (LSL)-mTmG mice (Meflin-ZDC; LSL-mTmG). In this model, all the recombined cells expressed membrane-localised green fluorescent protein (mGFP), allowing detailed visualisation of the entire morphology of the individual cells (**Supplementary material, Figure S6A**). It is noted that ZsGreen expression from the ZDC allele was so low in the pancreas that it did not affect the observation of mGFP fluorescence. Furthermore, we subjected the pancreas of Meflin-ZDC; LSL-mTmG to *in vivo* vascular staining by intravenous injection of an anti-CD31 antibody and isolectin B4, which binds to the endothelial cell surface [32,33], followed by tissue clearing [34] and three-dimensional (3D) observation by confocal microscopy (**Supplementary material, Figure S6B–D, Supplementary Movie 1, 2**). The data showed that most Meflin$^+$ PSCs extend their long and thin cytoplasmic protrusions on the abluminal surface of the capillary lumen. The

close association between the cytoplasmic protrusions of Meflin$^+$ PSCs and endothelial cells implies bidirectional crosstalk between these cells in the normal pancreas.

Meflin$^+$ PSCs are an origin of fibroblasts in CP and PDAC

To investigate the contribution of Meflin$^+$ PSCs to the fibrotic stromal reaction in CP and PDSC, we administered tamoxifen to Meflin-CreERT2; LSL-tdTomato mice, followed by CP induction by pancreatic duct ligation (PDL) or orthotopic transplantation of mouse PDAC cells [35] in the pancreas (**Figure 3A, F**). Given the specific labelling of Meflin$^+$ PSCs with tdTomato in the pancreas of Meflin-CreERT2; LSL-tdTomato mice (**Figure 2C, D**), this model allowed us to precisely trace the fate of Meflin$^+$ PSCs and their progeny. CP induction by PDL induced the activation of Meflin$^+$ PSC-derived cells localised around E-cadherin$^+$ epithelial cells that formed distorted ducts (**Figure 3B, C**). The Meflin$^+$ PSC-derived cells were positive for the pan-fibroblast marker platelet-derived growth factor receptor α (PDGFRα), demonstrating that the Meflin lineage is remarkably restricted to mesenchymal cells, including fibroblasts, and does not produce other lineages in the pancreas (**Figure 3D**). Given that tdTomato$^+$ cells comprised approximately 10% of PDGFRα$^+$ fibroblasts (**Figure 3E**) and that tdTomato-labelling efficiency in Meflin$^+$ PSCs was approximately 25% (**Figure 2E**), the contribution of Meflin$^+$ PSCs to fibroblast production should be higher than 10% and is estimated to be around 40% in CP. Similarly, we observed Meflin$^+$ PSC-derived cells between E-cadherin$^+$ tumour cells throughout the tumour stroma in the orthotopic PDAC (**Figure 3F–H**) [18]. Double IF staining for tdTomato and α-SMA, a myofibroblastic CAF (myCAF) marker [24], revealed that 25% of α-SMA$^+$ CAFs originated from Meflin$^+$ PSCs (**Figure 3I, J**). Taken together, these results indicate that Meflin$^+$ PSCs are one of the origins of fibroblasts in CP and PDAC.

Additionally, ISH analysis showed that approximately 18, 50, and 5% of Meflin$^+$ PSC-derived CAFs were positive for the inflammatory CAF (iCAF) marker *Il6*, myCAF marker *Acta2*, and antigen-presenting CAF (apCAF) marker *H2-Ab1*, respectively (**Supplementary**

material, Figure S7A, B) [24,36,37]. We then analysed the publicly available datasets of single-cell transcriptomic analysis of both mouse and human PDAC (GSE129455, GSE155698), and found that *Islr*$^{+}$ cells exhibited a different distribution from those of myCAFs, iCAFs, and apCAFs (**Supplementary material, Figure S7C, D**) [36,38]. These data suggest that Meflin^{+} PSC-derived CAFs and CAFs actively expressing Meflin (Meflin^{+} CAFs) are not identical to either myCAFs, iCAFs, and apCAFs, as we previously described [18,21,22,39,40].

Meflin^{+} PSC-derived fibroblasts show distinctive localisation and distribution in CP and PDAC when compared to normal pancreas

Given the close association of Meflin^{+} PSCs with the vasculature found in Meflin-ZDC; LSL-mTmG mice (**Supplementary material, Figure S6**), we investigated the changes in this association under diseased conditions. Therefore, we subjected Meflin-ZDC; LSL-tdTomato mice to CP and PDAC models, followed by *in vivo* vascular staining and tissue clearing (**Figure 4A, B**). Consistent with the findings in Meflin-ZDC; LSL-mTmG mice (**Supplementary material, Figure S6**), confocal microscopic analysis of the cleared pancreas showed that most tdTomato^{+} Meflin lineage cells were located adjacent to the vasculature in the normal pancreas (**Figure 4B**, upper panels, **Supplementary Movie 3, 4**). Interestingly, CP induction by PDL resulted in the formation of aberrant tortuous vessels surrounded by and interweaved with activated tdTomato^{+} Meflin lineage cells (**Figure 4B**, middle panel, **Supplementary Movie 5, 6**). Meflin lineage cells maintained their proximity to the vasculature under CP conditions. Furthermore, cellular distances to the nearest neighbour among tdTomato^{+} cells were shortened, indicating that tdTomato^{+} cells were distributed more densely in CP. (**Figure 4C**). Orthotopic transplantation of mT5 PDAC cells induced marked changes in the morphology and architecture of both vessels and tdTomato^{+} Meflin lineage cells (**Figure 4B**, lower panel, **Figure 4C, Supplementary Movie 7, 8**).

Specifically, tdTomato$^+$ Meflin lineage cells dissociated from flattened and dilated tumour vessels, and their cell size increased with multiple extended protrusions (**Figure 4B, C**).

Short-term Meflin$^+$ PSC depletion shows no evident effect in the normal pancreas

To obtain insights into the physiological functions of Meflin$^+$ PSCs, we depleted Meflin$^+$ PSCs by the intraperitoneal administration of diphtheria toxin (DTx) to adult Meflin-ZDC mice, which expresses the diphtheria toxin receptor under the Meflin promoter (**Supplementary material, Figure S8A**). Preliminary experiments showed that Meflin-ZDC mice became sick or moribund one week after DTx intraperitoneal administration. Therefore, we harvested pancreatic tissue samples five days after DTx administration, during which we observed a slight decrease in the mouse body weight (**Supplementary material, Figure S8B**). IHC for Desmin showed effective depletion of Desmin$^+$ PSCs in the group of Meflin-ZDC mice administered DTx (Meflin-ZDC mice, DTx+) when compared to control groups (Meflin-ZDC mice not administered DTx or wild-type mice administered DTx) (**Supplementary material, Figure S8C, D**). However, haematoxylin & eosin (H&E) staining revealed no changes in the histological architecture. Moreover, the effects on the vasculature and acinar cells were not evident, as assessed by IHC for CD31 and amylase, respectively. These data suggest that short-term depletion of Meflin$^+$ PSCs has no or only minor effects on tissue architecture and exocrine function in the normal pancreas.

Meflin$^+$ PSC depletion accelerates fibrosis and attenuates epithelial proliferative activity in CP

To examine the involvement of Meflin$^+$ PSCs in CP pathogenesis, we induced CP in Meflin-ZDC mice by PDL, followed by DTx intraperitoneal administration to deplete Meflin$^+$ PSCs (**Figure 5A**). While H&E staining showed no evident changes in the appearance of the epithelium, Sirus red and Masson's trichrome staining, IHC for type-I collagen and α-SMA,

and ISH for *Acta2* showed an increase in fibrosis in the stroma of the Meflin$^+$ PSC-depletion group (Meflin-ZDC mice, DTx+) when compared to the control groups (Meflin-ZDC mice, DTx− and wild-type mice, DTx+) (**Figure 5B, C, Supplementary material, S9A, B**). However, IHC for phospho-Smad2 showed no apparent association between TGF-β signalling and the fibrosis assessed by Sirus red and Masson's trichrome staining (**Supplementary material, Figure S9A, B**). There were also no significant differences between the groups in terms of the total area of the CD31$^+$ vascular lumen and the infiltration of CD45$^+$ leukocytes and CD11b$^+$ myeloid cells, except for the number of CD3$^+$ T cells that slightly increased in the Meflin$^+$ PSC-depletion group (**Supplementary material, Figure S9A, B**). We further investigated the regenerative potential of the pancreatic epithelium by evaluating the positivity of the cell proliferation marker Ki-67. The number of Ki-67$^+$ cells was significantly lower in the Meflin$^+$ PSC depletion group than in the control groups (**Figure 5B, C**).

Next, we explored the mechanism by which Meflin$^+$ PSC depletion affected the proliferative activity of the reparative epithelium. Histological analyses of the pancreas of Meflin knockout mice [17] in either normal or CP conditions showed no obvious alterations in fibrosis and epithelial proliferative activity when compared with wild-type mice (**Supplementary material, Figure S10A–D**). The results implied that the accelerated fibrosis and defect in epithelial regeneration induced by Meflin$^+$ PSC depletion could not be solely attributed to the loss of Meflin expression. Next, based on the established finding that the canonical Wnt signalling pathway is essential for regenerative epithelium proliferation upon tissue injury in various organs [41–43], we analysed the publicly available datasets of single-cell transcriptomic analysis of normal human pancreas and CP samples (EGAS00001004653) [44]. The data showed that Meflin$^+$ cells expressed R-spondin 3 (*Rspo3*), an R-spondin family member, which is known as a Wnt signalling enhancer (**Supplementary material, Figure S11A, B**) [45–47]. We confirmed this finding by ISH analysis on the CP tissues of Meflin-CreERT2; LSL-tdTomato mice, which showed that tdTomato$^+$ cells were positive for *Rspo3* (**Figure 6A**). Consistent with the role of Rspo3 in

enhancing Wnt signalling, E-cadherin$^+$ epithelial cells surrounded by tdTomato$^+$ cells robustly expressed *Axin2*, a universal readout of Wnt pathway activation (**Figure 6A**) [48]. Interestingly, the depletion of Meflin$^+$ PSCs in Meflin-ZDC mice following CP induction resulted in a significant decrease in *Axin2* expression and nuclear β-catenin expression, accompanied by a decrease in *Rspo3* expression in stromal cells (**Figure 6B, C**). These data suggest that Meflin$^+$ PSCs play a role in the promotion of epithelial regenerative responses by regulating Wnt signalling in CP conditions.

Finally, we examined the effect of Meflin$^+$ PSC depletion on PDAC pathogenesis. We orthotopically transplanted mT5 mouse PDAC cells into Meflin-ZDC mice, followed by an intraperitoneal injection of DTx (**Supplementary material, Figure S12A**). The results showed that Meflin$^+$ PSC depletion did not affect the number of Ki-67$^+$ cells, but decreased the expression levels of *Axin2* and *Rspo3* (**Supplementary material, Figure S12B, C**). The data suggested a conserved role of Meflin$^+$ PSCs or their lineage cells in the epithelial regenerative or proliferative responses between CP and PDAC conditions.

Discussion

The present study showed that Meflin is a PSC subset marker, which originates fibroblasts in CP and PDAC conditions in mice. Meflin$^+$ PSCs were close to the vasculature in the normal pancreas, whereas their distribution changed under disease conditions. Meflin$^+$ PSCs robustly expressed the Wnt signalling enhancer Rspo3, and depletion of Meflin$^+$ PSCs accelerated fibrosis and impaired epithelial regenerative response in CP.

As a PSC marker, Meflin has advantages over the conventional PSC markers, Desmin and GFAP, in terms of specificity, cross-species conservation, and applicability in *in vivo* experiments. Although Desmin is a PSC marker in rodents, it is also robustly expressed by vascular smooth muscles and does not label human PSCs in IHC [8,16]. GFAP also has difficulty detecting human PSCs using IHC [16]. In contrast, Meflin is expressed by not only

mouse PSCs, but also stromal cells in the human pancreas, although we should consider the limitation of the present study because we did not investigate whether Meflin$^+$ cells in the human pancreas possessed lipid droplets, a widely accepted hallmark of PSCs [1,6,7]. Furthermore, this new PSC marker provides an experimental platform based on the Cre-loxP system, enabling us to explore the fate of PSC lineage cells.

The localisation and morphology of Meflin$^+$ PSCs in 3D analyses have important implications for their functions. Meflin$^+$ PSCs, which seemed to be randomly located around the acini or ducts in two-dimensional tissue sections, were distributed mainly along the capillaries in the normal pancreas. This finding was consistent with a pioneer study using electron microscopy, which found vitamin A-storing cells in the perivascular regions [4,5]. Interestingly, we found that Meflin$^+$ PSCs had several long cellular protrusions clinging to capillaries. These observations implicate mechanical and functional interrelationships between Meflin$^+$ PSCs and capillaries, analogous to hepatic stellate cells and sinusoids in the liver [49,50]. Although we could not find any effects of short-term depletion of Meflin$^+$ PSC in the normal pancreas, the role of Meflin$^+$ PSCs in vascular function and homeostasis should be further investigated in detail in various models.

Meflin$^+$ PSCs produced fibroblasts under pathological conditions, such as CP and PDAC. The exact percentages of Meflin lineage cells in total fibroblasts were not determined in the present study, due to the relatively low labelling efficiency of Meflin$^+$ cells in our tamoxifen-inducible Cre mice. Gli1$^+$ fibroblasts produce approximately 50% of CAFs, and Fabp4$^+$ PSCs yield 10%–15% of CAFs [15,28,29]. Our previous study showed the heterogeneity of CAFs in human PDAC regarding Meflin and Gli1 expression; approximately 72%, 11%, and 17% of CAFs were Meflin$^+$Gli1$^+$, Meflin$^+$Gli1$^-$, and Meflin$^-$ Gli1$^+$, respectively [18]. We must interpret these data with caution because the proportional contributions of each origin could vary depending on the context, species, and individuals, and their gene expression patterns could change dynamically during disease progression. Nonetheless, these findings indicate that both PSCs and fibroblasts contribute to the production of activated heterogeneous fibroblasts in pancreatic diseases.

This study also provides two key findings that Meflin$^+$ PSCs contribute to tissue repair in pancreatic injury. First, Meflin$^+$ PSC depletion accelerated fibrosis in CP, suggesting the anti-fibrotic role of PSCs. Our previous study has shown that Meflin is expressed in CAFs in both mouse and human PDACs and suppresses fibrosis in PDAC stroma [18–22]. It has been demonstrated that PSCs play a crucial role in fibrosis through extracellular matrix production [8,9]; however, our previous and current results suggest that some subsets or transient states of PSCs may have anti-fibrotic roles in CP and PDAC. Second, Meflin$^+$ PSCs expressed the Wnt enhancer Rspo3, and their depletion affected epithelial regeneration in a CP mouse model. Given that the canonical Wnt pathway is essential for epithelial regeneration by supporting the proliferation of tissue stem cells or progenitors [41,42,51], Meflin$^+$ PSCs may support epithelial regeneration by producing Rspo3 in CP. However, an important caveat is that in the present study pancreatic tissues 12 days post PDL were assessed to avoid systemic toxicity of DTx administration in Meflin-ZDC mice, leaving the question open whether PSCs are primarily involved in regenerative and reparative or persistent fibrotic response after pancreatic injury. Interestingly, we and others previously found that Meflin is also expressed by fibroblasts in the heart, lung, kidney, and intestine, wherein it plays roles by providing protection against fibrosis and promoting tissue repair after tissue injuries [23,33,52,53]. Taken together with the present study, these studies will contribute to the understanding of the beneficial roles of fibroblasts in physiology and pathology.

In summary, Meflin is a marker of a PSC subset that originates fibroblasts in CP and PDAC. Meflin$^+$ PSCs have distinctive localisation and distribution in the normal and diseased pancreas, and are possibly involved in tissue recovery after pancreatic injury by suppressing fibrosis and supporting epithelial regeneration. Their possible role in controlling Wnt/Rspo signalling in PDAC context was also shown. We hope these findings shed new light on the importance of the morphology and functions of *in situ* tissue-resident PSCs, and provide a foundation for the future development of this research field.

Acknowledgements

We thank David Tuveson (Cold Spring Harbor Laboratory) and Chang-il Hwang (UC Davis College of Biological Sciences) for providing the mouse PDAC cells mT5; Minoru Tanaka, Kozo Uchiyama, Eri Yorifuji, and Yuya Yamaguchi (Nagoya University) and Kaori Ushida (Fujita Health University) for technical assistance.

Funding

This study was funded by the Japan Agency for Medical Research and Development (AMED) through grants 23gm1210009s0105 and 23ck0106779h0002 (to A.E.) and 23ck0106706h0003 (to T.I.), the Ministry of Education, Culture, Sports, Science, and Technology of Japan through grant 22H02848, 22K18390 (to A.E.), and 20H03467 (to M.T.), the Naito Foundation (to A.E.), the Takamatsunomiya Cancer Foundation (to A.E.), the DAIKO Foundation (to A.E.), and the Toyoaki Foundation (to A.E.). R.A. was supported by a Takeda Science Foundation Fellowship.

Author contributions

RA designed and performed the experiments, analysed the data, and wrote the manuscript. YS, YuM, HS, TI, YaM, and KI designed and performed the experiments and analysed the data. KF, ShuM, KK, and AK supported the experiments on tissue clearing and imaging. NA, ShiM, NE, and MT directed the project and provided intellectual input. AE directed the project and wrote the manuscript.

References

1. Apte MV, Pirola RC, Wilson JS. Fibrogenesis in the pancreas: The role of stellate cells. In *The Pancreas*, (3rd ed), Beger HG, Warshaw AL, Hruban RH et al. (eds). Wiley-Blackwell, 2018; 106–116.

2. Erkan M, Adler G, Apte MV, *et al.* StellaTUM: Current consensus and discussion on pancreatic stellate cell research. *Gut* 2012; **61**: 172–178.

3. Omary MB, Lugea A, Lowe AW, *et al.* The pancreatic stellate cell: A star on the rise in pancreatic diseases. *Journal of Clinical Investigation* 2007; **117**: 50–59.

4. Watari N, Hotta Y, Mabuchi Y. Morphological studies on a vitamin A-storing cell and its complex with macrophage observed in mouse pancreatic tissues following excess Vitamin A administration. *Okajimas Folia Anatomica Japonica* 1982; **58**: 837–857.

5. Ikejiri N. The Vitamin A-storing cells in the human and rat pancreas. *Kurume Medical J* 1990; **37**: 67–81.

6. Apte MV, Haber PS, Applegate TL, *et al.* Periacinar stellate shaped cells in rat pancreas: Identification, isolation, and culture. *Gut* 1998; **43**: 128–133.

7. Bachem MG, Schneider E, Groß H, *et al.* Identification, culture, and characterization of pancreatic stellate cells in rats and humans. *Gastroenterology* 1998; **115**: 421–432.

8. Haber PS, Keogh GW, Apte MV, *et al.* Activation of pancreatic stellate cells in human and experimental pancreatic fibrosis. *Am J Pathology* 1999; **155**: 1087–1095.

9. Apte MV, Park S, Phillips PA, *et al.* Desmoplastic reaction in pancreatic cancer. *Pancreas* 2004; **29**: 179–187.

10. Masamune A, Watanabe T, Kikuta K, *et al.* Roles of pancreatic stellate cells in pancreatic inflammation and fibrosis. *Clin Gastroenterol H* 2009; **7**: S48–S54.

11. Schnittert J, Bansal R, Prakash J. Targeting pancreatic stellate cells in cancer. *Trends Cancer* 2019; **5**: 128–142.

12. Neesse A, Bauer CA, Öhlund D, *et al.* Stromal biology and therapy in pancreatic cancer: Ready for clinical translation? *Gut* 2019; **68**: 159–171.

13. Sherman MH. Stellate cells in tissue repair, inflammation, and cancer. *Annu Rev Cell Dev Bi* 2018; **34**: 333–55.

14. Garcia PE, Scales MK, Allen BL, *et al.* Pancreatic fibroblast heterogeneity: From development to cancer. *Cells* 2020; **9**: 2464.

15. Sherman MH, Magliano MP di. Cancer-associated fibroblasts: Lessons from pancreatic cancer. *Annu Rev Cancer Biology* 2023; **7**.

16. Nielsen MFB, Mortensen MB, Detlefsen S. Identification of markers for quiescent pancreatic stellate cells in the normal human pancreas. *Histochem Cell Biol* 2017; **148**: 359–380.

17. Maeda K, Enomoto A, Hara A, *et al.* Identification of Meflin as a potential marker for mesenchymal stromal cells. *Sci Rep* 2016; **6**: 22288.

18. Mizutani Y, Kobayashi H, Iida T, *et al.* Meflin-positive cancer-associated fibroblasts inhibit pancreatic carcinogenesis. *Cancer Res* 2019; **79**: 5367–5381.

19. Iida T, Mizutani Y, Esaki N, *et al.* Pharmacologic conversion of cancer-associated fibroblasts from a protumor phenotype to an antitumor phenotype improves the sensitivity of pancreatic cancer to chemotherapeutics. *Oncogene* 2022; **41**: 2764–2777.

20. Takahashi M, Kobayashi H, Mizutani Y, *et al.* Roles of the mesenchymal stromal/stem cell marker Meflin/Islr in cancer fibrosis. *Frontiers Cell Dev Biology* 2021; **9**: 749924.

21. Ando R, Sakai A, Iida T, *et al.* Good and bad stroma in pancreatic cancer: Relevance of functional states of cancer-associated fibroblasts. *Cancers* 2022; **14**: 3315.

22. Shiraki Y, Mii S, Esaki N, *et al.* Possible disease-protective roles of fibroblasts in cancer and fibrosis and their therapeutic application. *Nagoya J Med Sci* 2022; **84**: 484–496.

23. Hara A, Kobayashi H, Asai N, *et al.* Roles of the mesenchymal stromal/stem cell marker Meflin in cardiac tissue repair and the development of diastolic dysfunction. *Circ Res* 2019; **125**: 414–430.

24. Öhlund D, Handly-Santana A, Biffi G, *et al.* Distinct populations of inflammatory fibroblasts and myofibroblasts in pancreatic cancer. *J Exp Med* 2017; **214**: 579–596.

25. Schaum N, Karkanias J, Neff NF, *et al.* Single-cell transcriptomics of 20 mouse organs creates a Tabula Muris. *Nature* 2018; **562**: 367–372.

26. Yamamoto G, Taura K, Iwaisako K, *et al.* Pancreatic Stellate Cells Have Distinct Characteristics From Hepatic Stellate Cells and Are Not the Unique Origin of Collagen-Producing Cells in the Pancreas. *Pancreas* 2017; **46**: 1141–1151

27. Baron M, Veres A, Wolock SL, *et al.* A Single-Cell Transcriptomic Map of the Human and Mouse Pancreas Reveals Inter- and Intra-cell Population Structure. *Cell Syst* 2016; **3**: 346–360.

28. Helms EJ, Berry MW, Chaw RC, *et al.* Mesenchymal Lineage Heterogeneity Underlies Non-Redundant Functions of Pancreatic Cancer-Associated Fibroblasts. *Cancer Discov* 2022; **12**: 484–501.

29. Garcia PE, Adoumie M, Kim EC, *et al.* Differential Contribution of Pancreatic Fibroblast Subsets to the Pancreatic Cancer Stroma. *Cell Mol Gastroenterology Hepatology* 2020; **10**: 581–599.

30. Apte MV, Pirola RC, Wilson JS. Pancreatic stellate cells. In *Stellate Cells in Health and Disease*, Chandrashekhar Gandhi and Massimo Pinzani (eds). Academic Press, 2015; 271–306.

31. Kisseleva T, Brenner D. Molecular and cellular mechanisms of liver fibrosis and its regression. *Nat Rev Gastroentero* 2021; **18**: 151–166.

32. Hirata Y, Furuhashi K, Ishii H, *et al.* CD150high bone marrow Tregs maintain hematopoietic stem cell quiescence and immune privilege via Adenosine. *Cell Stem Cell* 2018; **22**: 445–453.

33. Minatoguchi S, Saito S, Furuhashi K, *et al.* A novel renal perivascular mesenchymal cell subset gives rise to fibroblasts distinct from classic myofibroblasts. *Sci Rep* 2022; **12**: 5389.

34. Susaki EA, Tainaka K, Perrin D, *et al.* Advanced CUBIC protocols for whole-brain and whole-body clearing and imaging. *Nat Protoc* 2015; **10**: 1709–1727.

35. Boj SF, Hwang C-I, Baker LA, *et al.* Organoid models of human and mouse ductal pancreatic cancer. *Cell* 2015; **160**: 324–338.

36. Elyada E, Bolisetty M, Laise P, *et al.* Cross-species single-cell analysis of pancreatic ductal adenocarcinoma reveals antigen-presenting cancer-associated fibroblasts. *Cancer Discov* 2019; **9**: 1102–1123.

37. Menezes S, Okail MH, Jalil SMA, *et al.* Cancer-associated fibroblasts in pancreatic cancer: new subtypes, new markers, new targets. *J Pathol* 2022; **257**: 526–544.

38. Steele NG, Carpenter ES, Kemp SB, *et al.* Multimodal mapping of the tumor and peripheral blood immune landscape in human pancreatic cancer. *Nat Cancer* 2020; **1**: 1097–1112.

39. Miyai Y, Esaki N, Takahashi M, *et al.* Cancer-associated fibroblasts that restrain cancer progression: Hypotheses and perspectives. *Cancer Sci* 2020; **111**: 1047–1057.

40. Miyai Y, Sugiyama D, Hase T, *et al.* Meflin-positive cancer-associated fibroblasts enhance tumor response to immune checkpoint blockade. *Life Sci Alliance* 2022; **5**: e202101230.

41. Clevers H, Loh KM, Nusse R. An integral program for tissue renewal and regeneration: Wnt signaling and stem cell control. *Science* 2014; **346**: 1248012.

42. Nusse R, Clevers H. Wnt/β-Catenin signaling, disease, and emerging therapeutic modalities. *Cell* 2017; **169**: 985–999.

43. Huch M, Bonfanti P, Boj SF, *et al.* Unlimited in vitro expansion of adult bi-potent pancreas progenitors through the Lgr5/R-spondin axis. *Embo J* 2013; **32**: 2708–2721.

44. Tosti L, Hang Y, Debnath O, *et al.* Single-nucleus and in situ RNA-sequencing reveal cell topographies in the human pancreas. *Gastroenterology* 2021; **160**: 1330–1344.

45. Kazanskaya O, Glinka A, Barrantes I del B, *et al.* R-spondin2 is a secreted activator of Wnt/β-catenin signaling and is required for Xenopus myogenesis. *Dev Cell* 2004; **7**: 525–534.

46. Kazanskaya O, Ohkawara B, Heroult M, *et al.* The Wnt signaling regulator R-spondin 3 promotes angioblast and vascular development. *Development* 2008; **135**: 3655–3664.

47. Lau W de, Peng WC, Gros P, *et al.* The R-spondin/Lgr5/Rnf43 module: Regulator of Wnt signal strength. *Gene Dev* 2014; **28**: 305–316.

48. Lustig B, Jerchow B, Sachs M, *et al.* Negative feedback loop of wnt signaling through upregulation of Conductin/Axin2 in colorectal and liver tumors. *Mol Cell Biol* 2002; **22**: 1184–1193.

49. Gracia-Sancho J, Marrone G, Fernández-Iglesias A. Hepatic microcirculation and mechanisms of portal hypertension. *Nat Rev Gastroentero* 2019; **16**: 221–234.

50. Poisson J, Lemoinne S, Boulanger C, *et al.* Liver sinusoidal endothelial cells: Physiology and role in liver diseases. *J Hepatol* 2017; **66**: 212–227.

51. Kaestner KH. The intestinal stem cell niche – a central role for Foxl1-expressing subepithelial telocytes. *Cell Mol Gastroenterology Hepatology* 2019; **8**: 111–117.

52. Nakahara Y, Hashimoto N, Sakamoto K, *et al.* Fibroblasts positive for meflin have anti-fibrotic properties in pulmonary fibrosis. *Eur Respir J* 2021; **58**: 2003397.

53. Xu J, Tang Y, Sheng X, *et al.* Secreted stromal protein ISLR promotes intestinal regeneration by suppressing epithelial Hippo signaling. *EMBO J* 2020; **39**: e103255.

54. Watanabe S, Abe K, Anbo Y, *et al.* Changes in the mouse exocrine pancreas after pancreatic duct ligation: A qualitative and quantitative histological study. *Arch Histol Cytol* 1995; **58**: 365–374.

55. Xu X, D'Hoker J, Stangé G, *et al.* β cells can be generated from endogenous progenitors in injured adult mouse pancreas. *Cell* 2008; **132**: 197–207.

56. Nakajima C, Kamimoto K, Miyajima K, *et al.* A method for identifying mouse pancreatic ducts. *Tissue Eng Part C Methods* 2018; **24**: 480–485.

57. Ichihara R, Shiraki Y, Mizutani Y, *et al.* Matrix remodeling-associated protein 8 is a marker of a subset of cancer-associated fibroblasts in pancreatic cancer. *Pathol Int* 2022; **72**: 161–175.

58. Saito M, Iwawaki T, Taya C, *et al.* Diphtheria toxin receptor–mediated conditional and targeted cell ablation in transgenic mice. *Nat Biotechnol* 2001; **19**: 746–750.

59. Hao Y, Hao S, Andersen-Nissen E, *et al.* Integrated analysis of multimodal single-cell data. *Cell* 2021; **184**: 3573–3587.

References 54–59 are cited only in the supplementary material.

Figure legends

Figure 1. Meflin (*Islr*) is expressed in stromal cells of both mouse and human pancreas.

(A) Tissue sections from the normal mouse pancreas were stained for *Islr* by *in situ* hybridisation (ISH) (left) and Desmin by immunohistochemistry (IHC) (right). Both $Islr^+$ and $Desmin^+$ cells were present in the periacinar, periductal, perivascular, and periislet regions (arrowheads). Arrows denote $Desmin^+$ vascular smooth muscle cells. Boxed areas **(a–d)** were magnified in lower panels. IL, islet of Langerhans; D, duct; V, vessel; Ac, acinus. Scale bar: 50 µm.

(B, C) Tissue sections from the normal mouse pancreas were double stained for *Islr* by ISH (green) and Desmin by immunofluorescence (magenta) **(B)**, followed by quantification of *Islr* and Desmin (Des) co-expression (n = 25 images from five mice) **(C)**. The white arrowhead indicates a double-positive cell. Scale bar: 10 µm.

(D, E) Primary cultured PSCs isolated from mouse pancreas by density gradient centrifugation were stained for *Islr* by ISH (green) **(D)**, followed by quantification of the number of cells positive for *Islr* (n = 3 mice), lipid droplets (n = 5 mice), and Desmin (n = 5 mice). **(E)**. Scale bar: 10 µm.

(F) Tissue sections from the normal human pancreas were stained for *ISLR* by ISH (left panel), Meflin by IHC (middle panel), and Desmin by IHC (right panel). Boxed areas were magnified in lower panels. $ISLR^+$ or $Meflin^+$ cells were observed in the interstitium of the pancreas (arrowheads), while Desmin expression were found only in vascular smooth muscle cells (arrows). Scale bar: 50 µm.

Figure 2. Meflin-CreERT2 knock-in mouse specifically labels pancreatic stellate cells.

(A) Schematic diagram of the experimental protocol using Meflin-CreERT2; LSL-tdTomato mice. $Meflin^+$ cells were labelled by tdTomato upon tamoxifen administration.

(B) Tissue sections from the pancreas of adult Meflin-CreERT2; LSL-tdTomato mice administered tamoxifen were stained for tdTomato by immunohistochemistry. Arrowheads indicate tdTomato$^+$ cells in the interstitium around acini or islets. IL, islet of Langerhans; D, duct; V, vessel; Ac, acinus. Scale bar: 50 μm.

(C–E) The same sections described above were double stained for *Islr* by *in situ* hybridisation (ISH) and tdTomato by immunofluorescence (IF) **(C)**, followed by quantification (n = 30 images from three mice) **(D, E)**. Most tdTomato$^+$ cells were positive for *Islr*, confirming the specificity of the Meflin reporter mice **(D)**. The labelling efficiency of the reporter mice was determined at approximately 25% **(E)**. The white arrowhead indicates a double-positive cell. Scale bar: 10 μm.

(F, G) The same sections described above were double stained for the indicated antibodies **(F)**, and double positivity was quantified **(G)** (n = 20–25 images from 4–5 mice). The white arrowhead indicates a double-positive cell. Scale bar: 10 μm.

(H, I) tdTomato$^+$ cells dissociated from the pancreas of Meflin-CreERT2; LSL-tdTomato mice (n = 4) administered tamoxifen were stained by BODIPY 493/503 (green) to examine the presence of lipid droplets **(H)**, followed by quantification **(I)**. Scale bar: 20 μm.

(J, K) Tissue section from the pancreas of adult Meflin-CreERT2; LSL-tdTomato mice administered tamoxifen were double stained for tdTomato (magenta) and Fabp4 (green) by IF **(J)**, followed by quantification (n = 25 images from five mice) **(K)**. Scale bar: 10 μm.

(L, M) Sections of the mouse pancreas were double stained for *Islr* (magenta) and *Gli1* (green) by ISH **(L)**, followed by quantification (n = 37 images from three mice) **(M)**. Scale bar: 10 μm.

(N) A Venn diagram showing the overlap between *Islr*$^+$, *Gli1*$^+$, and Fapb4$^+$ stromal cells in the normal mouse pancreas.

Figure 3. Meflin$^+$ pancreatic stellate cells are an origin of fibroblasts in chronic pancreatitis (CP) and pancreatic ductal adenocarcinoma (PDAC).

(A) Schematic diagram of the experiment. Meflin-CreERT2; LSL-tdTomato mice were orally administered tamoxifen on days 0, 2, and 4, followed by pancreatic duct ligation (PDL) to induce CP on day 14. The mice were fixed four weeks after PDL.

(B) Tissue sections from the pancreas of Meflin-CreERT2; LSL-tdTomato mice that underwent CP induction were stained for tdTomato by immunohistochemistry (IHC), showing spindle-shaped activated tdTomato$^+$ cells were localised around distorted ducts. Scale bar: 50 μm.

(C–E) The same sections described above were double stained for tdTomato (magenta) and E-cadherin or PDGFRα (green) by immunofluorescence (IF) **(C, D)**, followed by quantification of tdTomato and PDGFRα positivity (n = 25 images from five mice) **(E)**. Scale bar: 50 μm.

(F) Meflin-CreERT2; LSL-tdTomato mice were orally administered tamoxifen, followed by orthotopic mT5 PDAC cell transplantation.

(G–I) Tissue sections from the orthotopically transplanted PDAC in Meflin-CreERT2; LSL-tdTomato mice were stained for tdTomato by IHC **(G)** or double stained for tdTomato and E-cadherin or α-SMA by IF **(H, I)**. Note that tdTomato$^+$ cells proliferated around E-cadherin$^+$ epithelial cells and merged with a cancer-associated fibroblast (CAF) marker α-SMA. **(J)** Quantification of tdTomato and α-SMA positivity in the experiments (n = 30 images from three mice). Scale bar: 50 μm.

Figure 4. Meflin$^+$ pancreatic stellate cell-derived fibroblasts show distinctive localisation and distribution in chronic pancreatitis (CP) and pancreatic ductal adenocarcinoma (PDAC) when compared to normal pancreas.

(A) Meflin-ZDC (ZsGreen-T2A-diphtheria toxin receptor [DTR]-T2A-Cre); LSL-tdTomato mice were subjected to CP and PDAC models by pancreatic duct ligation (PDL) and orthotopic mT5 PDAC cell transplantation, respectively, followed by *in vivo* vascular staining, isolation of pancreas, tissue clearing, and imaging of 3D morphology of Meflin$^+$ PSCs.

(B) 3D images of cleared pancreatic tissues from the normal pancreas of Meflin-ZDC; LSL-tdTomato mice (upper panels), and those subjected to the CP model (middle panels) and the PDAC model (lower panels). Scale bars = 50 μm.

(C) Quantification of the distances between tdTomato$^+$ Meflin lineage cells to the nearest tdTomato$^+$ cells or capillaries. Meflin lineage cells localised closer to and farther from the capillaries in CP and PDAC, respectively, when compared to the normal pancreas. Two-sided nonparametric Brunner–Munzel test was performed to test the statistical significance of differences between the groups.

Figure 5. Meflin$^+$ pancreatic stellate cell (PSC) depletion accelerates fibrosis and attenuates epithelial proliferative activity in chronic pancreatitis (CP).

(A) Schematic diagram of the PSC depletion experiment in CP. Meflin-ZDC (ZsGreen-T2A-diphtheria toxin receptor [DTR]-T2A-Cre) mice were subjected to pancreatic duct ligation (PDL) to induce CP, followed by intraperitoneal administration of diphtheria toxin (DTx) and isolation of pancreata one day after the last dose of DTx. Meflin-ZDC mice not administered DTx and wild-type mice administered DTx served as controls.

(B, C) Tissue sections from the pancreata were examined by H&E, Sirius red and Masson's trichrome staining, immunohistochemistry for type I collagen and α-SMA, and immunofluorescence for Ki-67 and E-cadherin **(B)**, followed by quantification of Sirius red$^+$, Masson's trichrome$^+$, type I collagen$^+$ and α-SMA$^+$ areas, and the number of Ki-67$^+$ cells (n = 35 images from seven mice/group, *t*-tests, Bonferroni adjusted P values) **(C)**. The data

showed that the depletion of Meflin$^+$ PSCs resulted in more advanced fibrosis of the stroma and a decrease in the number of Ki-67$^+$ cells.

Figure 6. Meflin lineage cells express *Rspo3* and support epithelial Wnt signalling in chronic pancreatitis (CP).

(A) Tissue sections from CP induced in Meflin-CreERT2; LSL-tdTomato mice were triple-stained for tdTomato (magenta) and E-cadherin (white) by immunofluorescence (IF) and *Rspo3* (left) or *Axin2* (right) by *in situ* hybridisation (ISH) (green). Note that E-cadherin$^+$ epithelial cells were positive for *Axin2* (green arrowheads), whereas *Rspo3* was positive in tdTomato$^+$ Meflin lineage cells localised adjacent to the E-cadherin$^+$ epithelial cells (white arrowheads). Scale bar = 10 μm.

(B, C) Meflin-ZDC (ZsGreen-T2A-diphtheria toxin receptor [DTR]-T2A-Cre) mice were subjected to pancreatic duct ligation to induce CP, followed by the depletion of Meflin$^+$ PSCs by intraperitoneal administration of diphtheria toxin (DTx). Tissue sections from isolated pancreata were stained for *Rspo3* and *Axin2* by ISH, E-cadherin by IF, and β-catenin by immunohistochemistry **(B)**, followed by quantification (n = 35 pictures from 7 mice/group, *t*-tests, Bonferroni adjusted P values) **(C)**. Meflin$^+$ PSC depletion reduced *Rspo3*$^+$ areas, accompanied by a decrease in the *Axin2*$^+$ and nuclear β-catenin$^+$ areas. Scale bar = 50 μm.

List of supplemental materials online

1. Supplementary materials and methods

2. Supplementary figures

Figure S1. Expression of Meflin (*Islr*) in stromal cells positive for Desmin and lipid droplets in the pancreas.

Figure S2. Sparse localisation of Meflin$^+$ cells in the smooth muscle cell layer of vessels in the pancreas.

Figure S3. Meflin$^+$ cells possess the ability to uptake exogenous retinol (vitamin A).

Figure S4. Meflin does not label the majority of hepatic stellate cells (HSCs) in the liver.

Figure S5. Meflin-constitutive Cre knock-in mouse labels pancreatic stellate cells.

Figure S6. Morphology of Meflin lineage cells (Meflin$^+$ pancreatic stellate cells) and their perivascular localisation in the normal mouse pancreas.

Figure S7. Meflin$^+$ pancreatic stellate cells yield both inflammatory cancer-associated fibroblasts (iCAFs) and myofibroblastic CAFs (myCAFs) in the pancreatic ductal adenocarcinoma (PDAC) mouse model.

Figure S8. Short-term Meflin$^+$ pancreatic stellate cell depletion shows no evident effect in the normal pancreas.

Figure S9. Effects of Meflin$^+$ pancreatic stellate cell depletion on *Acta2* expression, Smad2 activation, vascular lumen area, and immune cell infiltration in chronic pancreatitis.

Figure S10. No apparent differences in fibrosis and epithelial proliferation between wild-type and Meflin-knockout (KO) mice in both normal and chronic pancreatitis (CP) conditions.

Figure S11. *Rspo3* is specifically expressed by Meflin$^+$ pancreatic stellate cells (PSCs) in the normal human pancreas and human chronic pancreatitis (CP).

Figure S12. Effects of Meflin$^+$ pancreatic stellate cell depletion on the number of Ki-67+ cells and Rspo3 and Axin2 expression in the pancreatic ductal adenocarcinoma (PDAC) mouse model.

3. Supplementary movies

Movie 1. Animation of a confocal Z-stack image series of a tissue section obtained from the normal pancreas of Meflin-ZDC; LSL-mTmG mouse. Red, E-cadherin; Green, Meflin lineage cells; White, vessels.

Movie 2. Animation of 3D reconstruction of a confocal image series of a tissue section obtained from the normal pancreas of Meflin-ZDC; LSL-mTmG mouse. 3D images created with surface rendering were also shown. Green, Meflin lineage cells; White, vessels.

Movie 3. Animation of a confocal Z-stack image series of a tissue section obtained from the normal pancreas of Meflin-ZDC; LSL-tdTomato mouse. Red, Meflin$^+$ cells; White, vessels; Blue, nuclei.

Movie 4. Animation of 3D reconstruction of a confocal image series of a tissue section obtained from the normal pancreas of Meflin-ZDC; LSL-tdTomato mouse. 3D images created with surface rendering were also shown. Red, Meflin lineage cells; White, vessels.

Movie 5. Animation of a confocal Z-stack image series of a tissue section obtained from chronic pancreatitis tissue of Meflin-ZDC; LSL-tdTomato mouse. Red, Meflin lineage cells; White, vessels; Blue, nuclei.

Movie 6. Animation of 3D reconstruction of a confocal image series of a tissue section obtained from chronic pancreatitis tissue of Meflin-ZDC; LSL-tdTomato mouse. 3D images created with surface rendering were also shown. Red, Meflin lineage cells; White, vessels.

Movie 7. Animation of a confocal Z-stack image series of a tissue section obtained from a PDAC tumor developed in Meflin-ZDC; LSL-tdTomato mouse. Red, Meflin lineage cells; White, vessels; Blue, nuclei.

Movie 8. Animation of 3D reconstruction of a confocal image series of a tissue section obtained from a PDAC tumor developed in Meflin-ZDC; LSL-tdTomato mouse. 3D images created with surface rendering were also shown. Red, Meflin lineage cells; White, vessels.

Figure 1

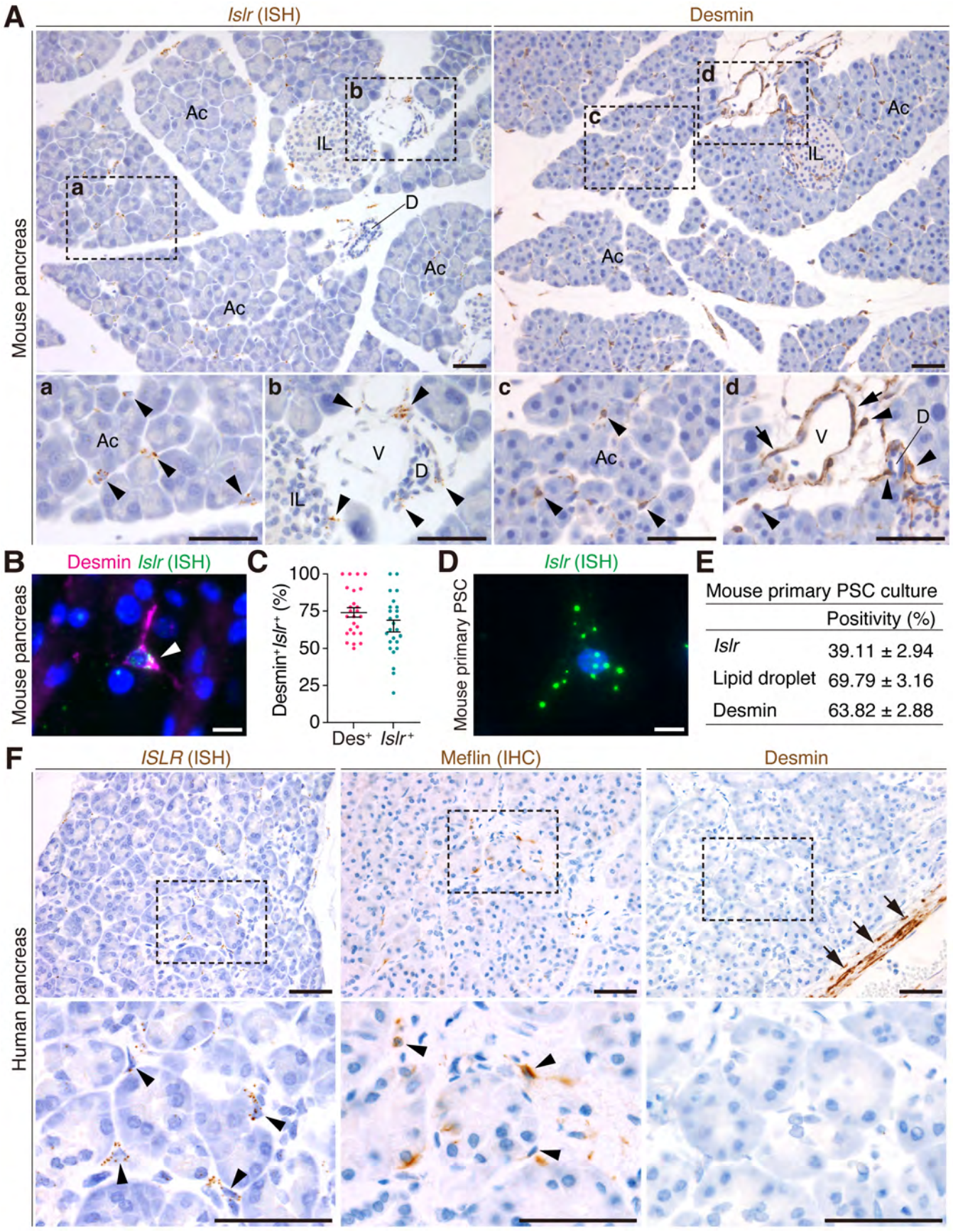
A
Islr (ISH)
Desmin
Mouse pancreas
Ac
IL
D
V
a
b
c
d
B
Desmin Islr (ISH)
Mouse pancreas
C
Desmin+Islr+ (%)
100
75
50
25
0
Des+
Islr+
D
Islr (ISH)
Mouse primary PSC
E
Mouse primary PSC culture
Positivity (%)
Islr 39.11 ± 2.94
Lipid droplet 69.79 ± 3.16
Desmin 63.82 ± 2.88
F
ISLR (ISH)
Meflin (IHC)
Desmin
Human pancreas

Figure 2

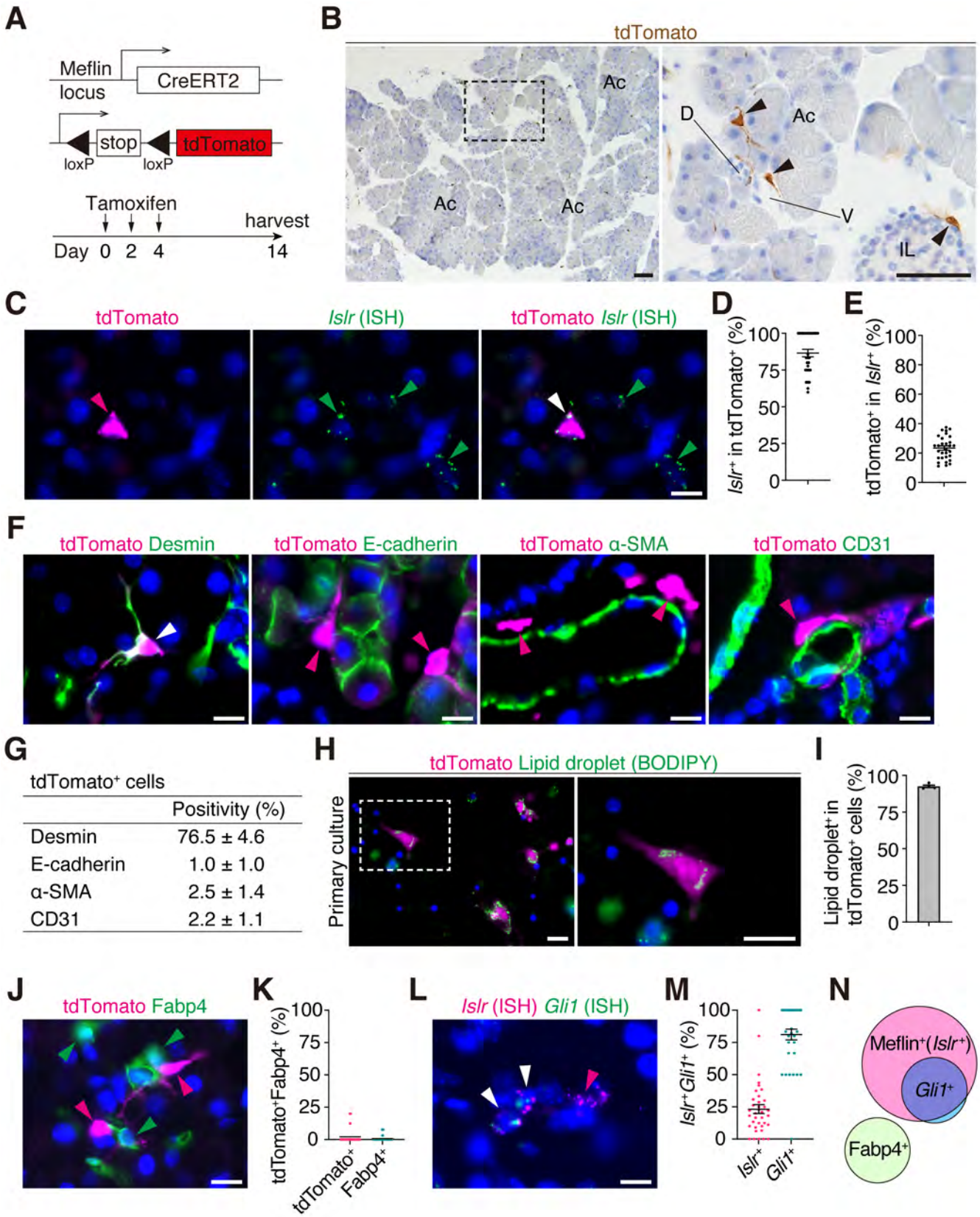
A
Meflin locus
CreERT2
stop
tdTomato
loxP
loxP
Tamoxifen
Day 0 2 4
harvest
14
B
tdTomato
Ac
Ac
Ac
D
V
IL
C
tdTomato
Islr (ISH)
tdTomato Islr (ISH)
D
Islr+ in tdTomato+ (%)
100
75
50
25
0
E
tdTomato+ in Islr+ (%)
100
80
60
40
20
0
F
tdTomato Desmin
tdTomato E-cadherin
tdTomato α-SMA
tdTomato CD31
G
tdTomato+ cells
Positivity (%)
Desmin 76.5 ± 4.6
E-cadherin 1.0 ± 1.0
α-SMA 2.5 ± 1.4
CD31 2.2 ± 1.1
H
tdTomato Lipid droplet (BODIPY)
Primary culture
I
Lipid droplet+ in tdTomato+ cells (%)
100
75
50
25
0
J
tdTomato Fabp4
K
tdTomato+Fabp4+ (%)
100
75
50
25
0
tdTomato+
Fabp4+
L
Islr (ISH) Gli1 (ISH)
M
Islr+Gli1+ (%)
100
75
50
25
0
Islr+
Gli1+
N
Meflin+(Islr+)
Gli1+
Fabp4+

Figure 3

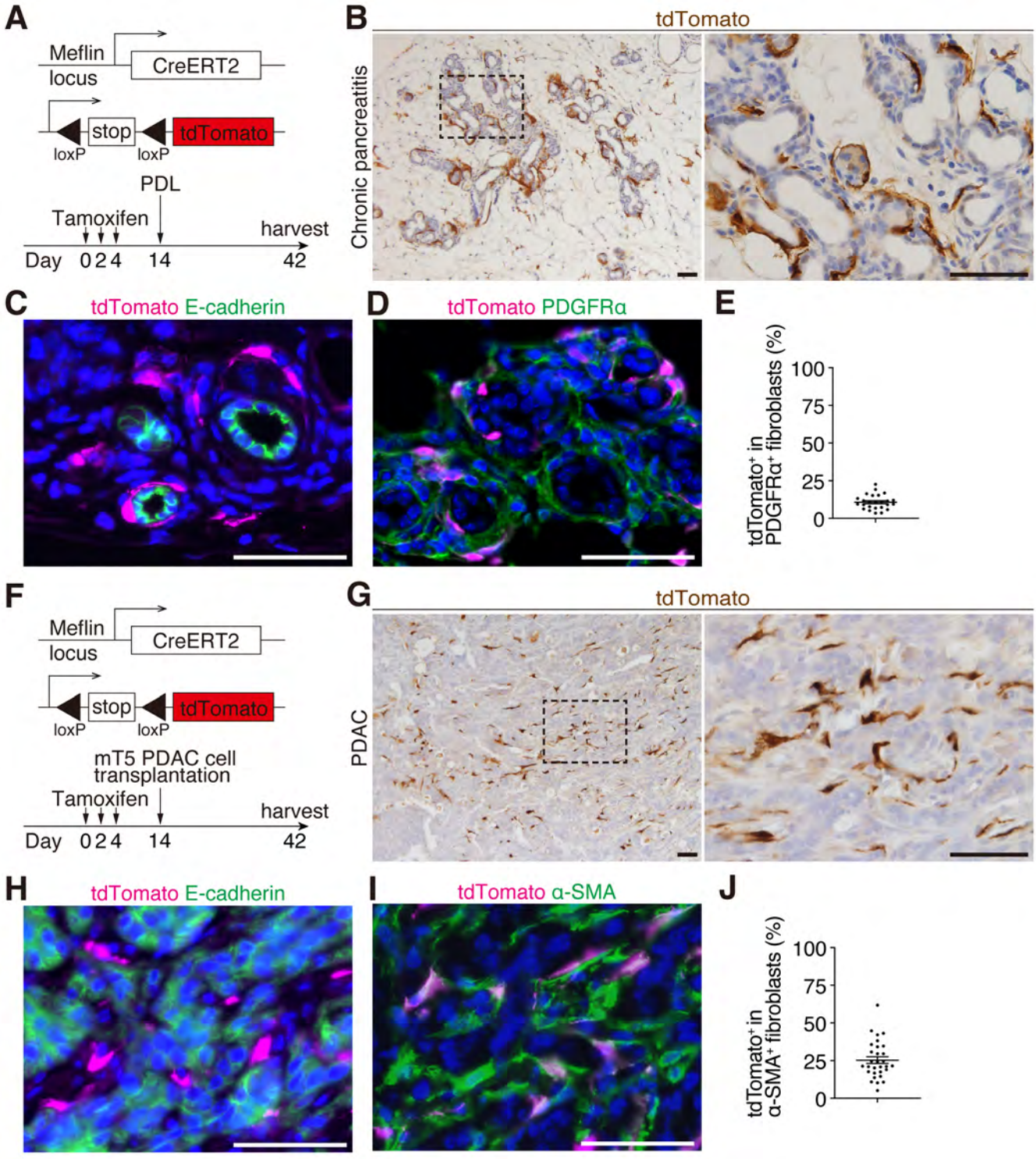
A
Meflin locus
CreERT2
stop
tdTomato
loxP
loxP
PDL
Tamoxifen
harvest
Day 0 2 4 14 42
B
tdTomato
Chronic pancreatitis
C
tdTomato E-cadherin
D
tdTomato PDGFRα
E
tdTomato+ in PDGFRα+ fibroblasts (%)
100
75
50
25
0
F
Meflin locus
CreERT2
stop
tdTomato
loxP
loxP
mT5 PDAC cell transplantation
Tamoxifen
harvest
Day 0 2 4 14 42
G
tdTomato
PDAC
H
tdTomato E-cadherin
I
tdTomato α-SMA
J
tdTomato+ in α-SMA+ fibroblasts (%)
100
75
50
25
0

Figure 4

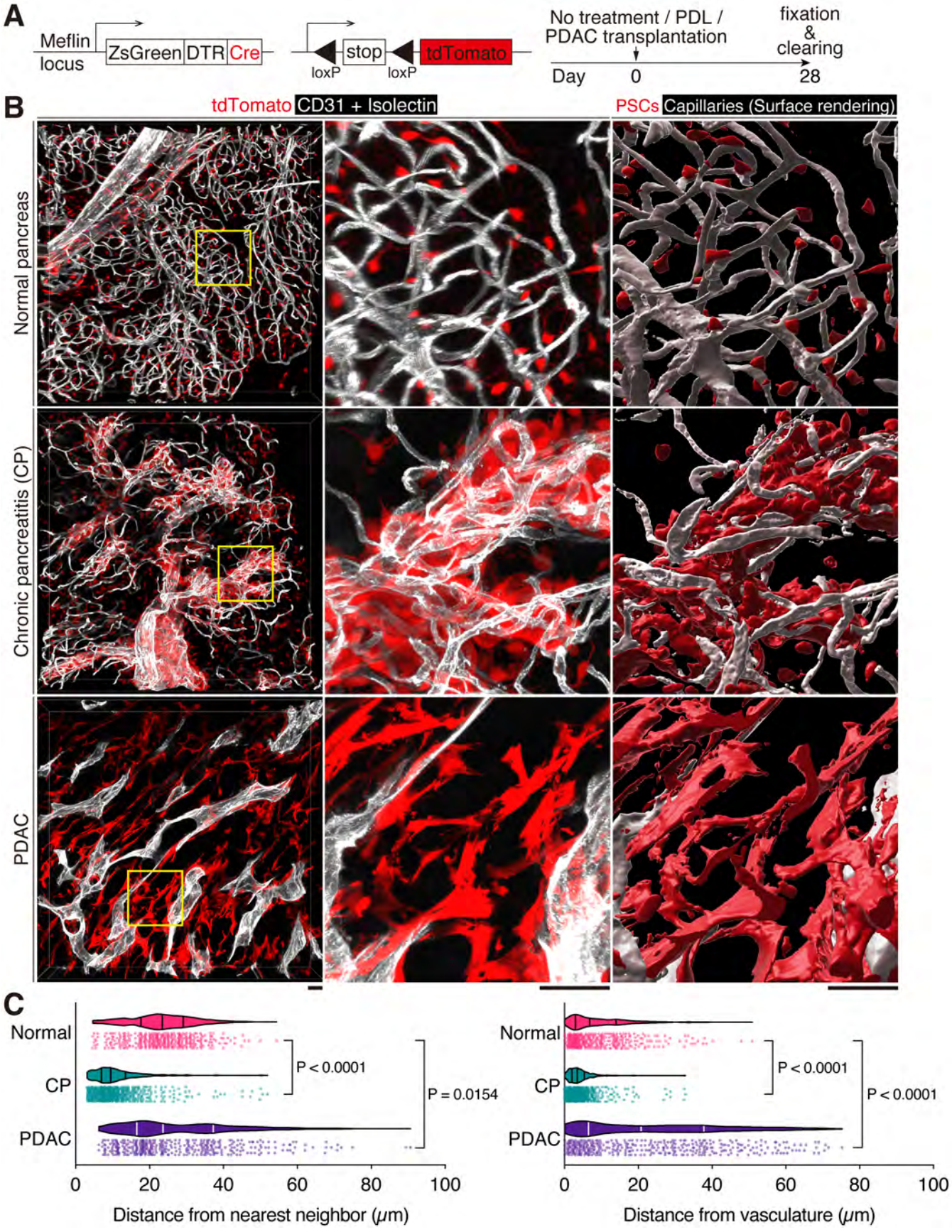
A
Meflin locus
ZsGreen
DTR
Cre
loxP
stop
loxP
tdTomato
No treatment / PDL / PDAC transplantation
fixation & clearing
Day
0
28
B
tdTomato CD31 + Isolectin
PSCs Capillaries (Surface rendering)
Normal pancreas
Chronic pancreatitis (CP)
PDAC
C
Normal
CP
PDAC
P < 0.0001
P = 0.0154
0
20
40
60
80
100
Distance from nearest neighbor (μm)
Normal
CP
PDAC
P < 0.0001
P < 0.0001
0
20
40
60
80
100
Distance from vasculature (μm)

Figure 5

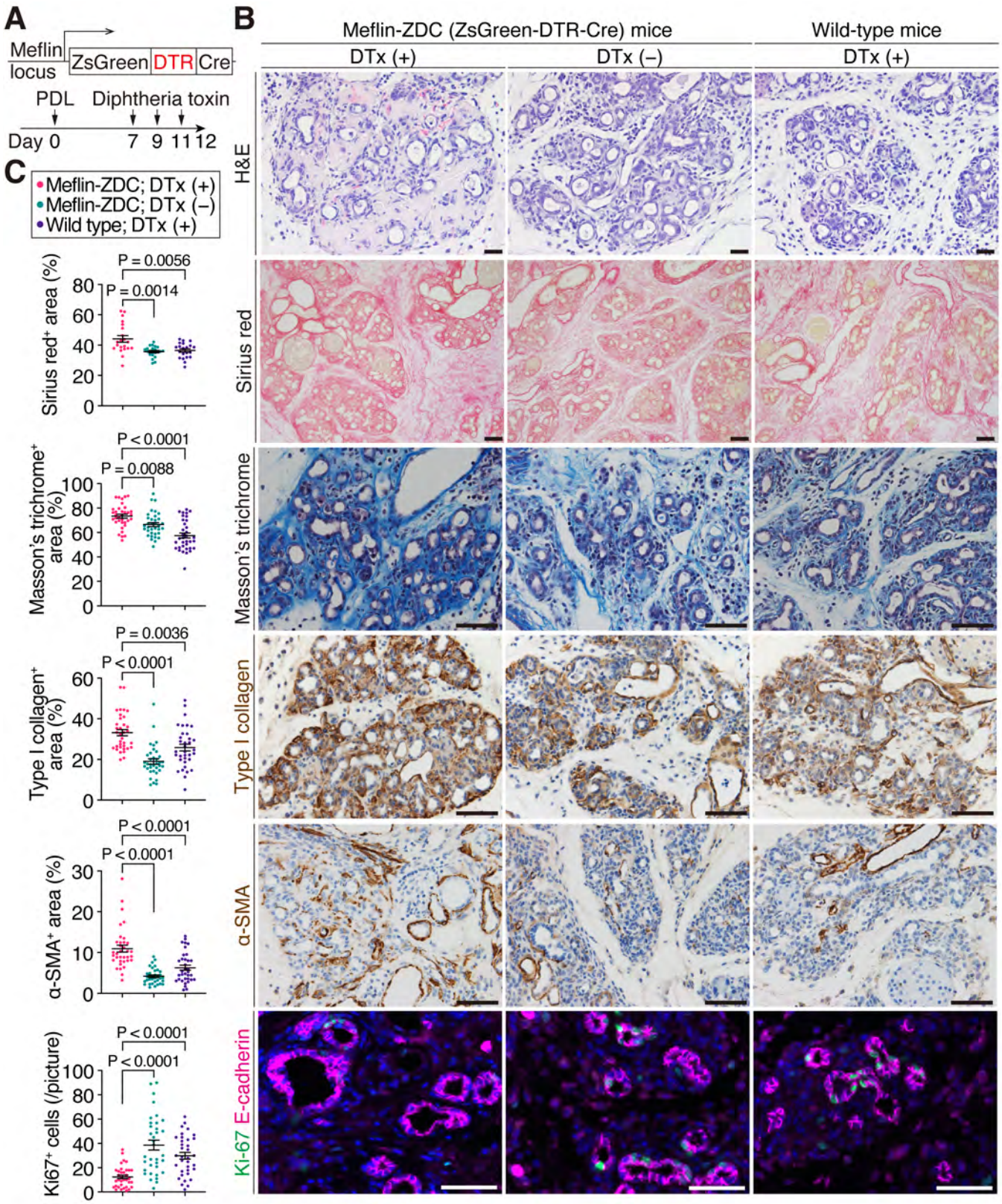
A
Meflin locus
ZsGreen
DTR
Cre
PDL
Diphtheria toxin
Day 0
7 9 11 12
B
Meflin-ZDC (ZsGreen-DTR-Cre) mice
Wild-type mice
DTx (+)
DTx (–)
DTx (+)
H&E
Sirius red
Masson's trichrome
Type I collagen
α-SMA
Ki-67 E-cadherin
C
Meflin-ZDC; DTx (+)
Meflin-ZDC; DTx (–)
Wild type; DTx (+)
Sirius red+ area (%)
P = 0.0056
P = 0.0014
Masson's trichrome+ area (%)
P < 0.0001
P = 0.0088
Type I collagen+ area (%)
P = 0.0036
P < 0.0001
α-SMA+ area (%)
P < 0.0001
P < 0.0001
Ki67+ cells (/picture)
P < 0.0001
P < 0.0001

Figure 6

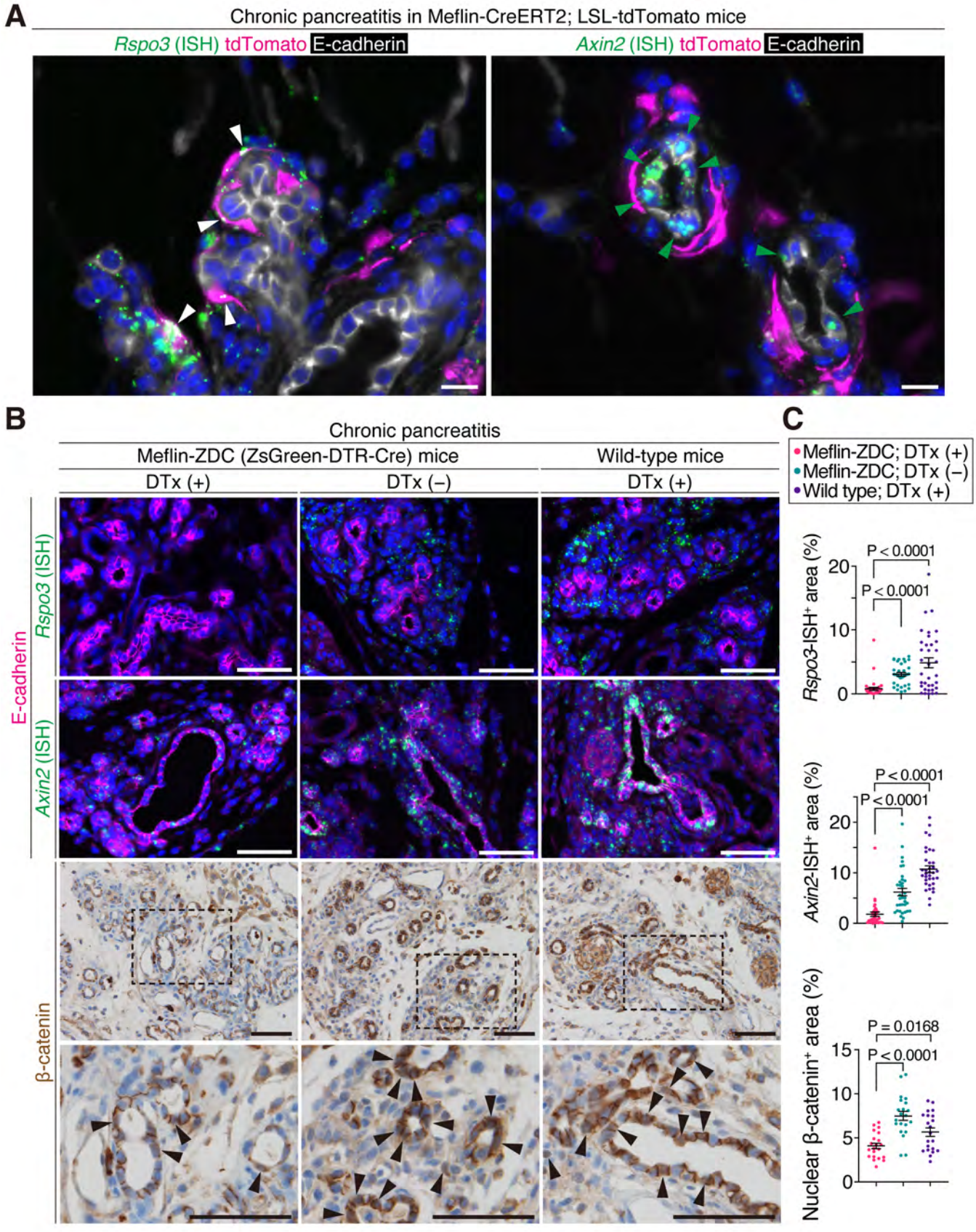
A
Chronic pancreatitis in Meflin-CreERT2; LSL-tdTomato mice
Rspo3 (ISH) tdTomato E-cadherin
Axin2 (ISH) tdTomato E-cadherin
B
Chronic pancreatitis
Meflin-ZDC (ZsGreen-DTR-Cre) mice
Wild-type mice
DTx (+)
DTx (–)
DTx (+)
E-cadherin
Rspo3 (ISH)
Axin2 (ISH)
β-catenin
C
Meflin-ZDC; DTx (+)
Meflin-ZDC; DTx (–)
Wild type; DTx (+)
Rspo3-ISH+ area (%)
P < 0.0001
P < 0.0001
Axin2-ISH+ area (%)
P < 0.0001
P < 0.0001
Nuclear β-catenin+ area (%)
P = 0.0168
P < 0.0001